Lithospheric Structure of the Arabian Shield and Platform from Complete Regional Waveform Modeling and Surface Wave Group Velocities

Arthur J. Rodgers, William R. Walter

Lawrence Livermore National Laboratory, Geophysics and Global Security Division, Livermore, CA, USA

Robert J. Mellors

San Diego State University, Department of Geological Sciences, San Diego, CA, USA

Abdullah M. S. Al-Amri

King Saud University, Geophysical Observatory, Riyadh, Kingdom of Saudi Arabia

and

Yu-Shen Zhang

University of California, Santa Cruz, Institute of Tectonics, Santa Cruz, CA, USA

Manuscript in press *Geophysical Journal International*

Submitted October, 1998

Revised April, 1999

Keywords: Waveform analysis, lithosphere, crustal structure, surface waves

Short title: Arabian lithospheric structure

Summary

Regional seismic waveforms reveal significant differences in the structure of the Arabian Shield and the Arabian Platform. We estimate lithospheric velocity structure by modeling regional waveforms recorded by the 1995-1997 Saudi Arabian Temporary Broadband Deployment using a grid search scheme. We employ a new method whereby we narrow the waveform modeling grid search by first fitting the fundamental mode Love and Rayleigh wave group velocities. The group velocities constrain the average crustal thickness and velocities as well as crustal velocity gradients. Because the group velocity fitting is computationally much faster than the synthetic seismogram calculation this method allows us to quickly determine good average starting models. Waveform fits of the Pn and Sn body wave arrivals constrain mantle velocities. Resulting lithospheric structures indicate that the Arabian Platform has an average crustal thickness of 40 km with relatively low crustal velocities (average crustal P- and S-wave velocities of 6.07 km/s and 3.50 km/s, respectively) without a strong velocity gradient. The Moho is shallower (36 km) and crustal velocities are 6% higher (with a velocity increase with depth) for the Arabian Shield. Fast crustal velocities of the Arabian Shield result from a predominately mafic composition in the lower crust. Lower velocities in the Arabian Platform crust indicate a bulk felsic composition, consistent with orogenesis of this former active margin. P- and S-wave velocities immediately below the Moho are slower in the Arabian Shield than in the Arabian Platform (7.9 km/s and 4.30 km/s and 8.10 km/s and 4.55 km/s, respectively). This indicates that the Poisson's ratios for the Arabian Shield and Platform uppermost mantle are 0.29 and 0.27, respectively. The lower mantle velocities and higher Poisson's ratio beneath the Arabian Shield likely arise from a partially molten mantle associated with Red Sea spreading and continental volcanism, although we cannot constrain the lateral extent of a zone of partially molten mantle.

Introduction

The Arabian Peninsula is composed of the (western) Arabian Shield and the (eastern) Arabian Platform (Figure 1). Several distinct terranes make up the Shield with the eastern terranes having continental affinity and the western terranes having island arc affinity (Stoeser and Camp, 1985). Unlike most continental shield regions, the Arabian Shield contains areas of recent volcanism. Locations of Neogene-Quaternary basalt cover, related to recent continental volcanic activity, are shown in Figure 1. Camp and Roobol (1992) analyzed rocks from these sites and found evidence for two episodes of volcanism. They concluded that the more recent phase of volcanic activity (12 Ma to present) is related to active mantle upwelling contemporaneous with uplift of western Arabia. The Arabian Platform shows no volcanic activity. Proterozoic basement is exposed in the shield, however the platform is covered by Phanerozoic sediments which gradually thicken (west-to-east) to nearly 10 km in the Mesopotamian Foredeep and Arabian Gulf (Seber et al., 1997). Eastward oceanic subduction and collision of continental terranes led to orogenesis along the western margin of the Arabian Platform in Late Proterozoic times (Stoeser and Camp, 1985). The Arabian Gulf is underlain by continental crust which is currently colliding with the Eurasian Plate along the Zagros Thrust.

A seismic refraction profile conducted in the Arabian Shield (Gettings et al., 1986) is roughly coincident with the temporary broadband stations SODA, RANI, HALM, RAYN & RIYD (Figure 1). These data revealed a 40 km thick crust in the central shield with average velocities of 6.3 km/s for the upper crust and 7.0 km/s for the lower crust and a mid-crustal reflector at about 20 km depth (Gettings et al., 1986). That study also reported that the crust rapidly thins near the Red Sea. An interesting observation is that the topography is higher on average in the western Arabian Shield than in central Arabia, despite the inferred thinner crust. Al-Amri (1998, 1999) modeled P-wave spectra to infer crustal structure near the seismic observatory in Riyadh (a long-period analog station near RIYD, Figure 1). He reported fast crustal velocities, consistent with the refraction results. Regional surface wave investigations of the Arabian Peninsula revealed variations in shear

wave velocity and attenuation structure. Seber and Mitchell (1992) modeled short-period (5-30 s) fundamental mode Love and Rayleigh wave spectra to estimate shear wave velocity and attenuation of the upper crust. They concluded that Q_S in the upper crust is generally low throughout Arabia with values of 60 for western Arabia, 100-150 for central Arabia and 65-85 for eastern Arabia. Mokhtar and Al-Saeed (1994) inverted Love and Rayleigh wave group velocity curves observed at RYD to estimate shear wave velocity structure for paths from the Red Sea, Gulf of Aden and Zagros. They found paths from the Red Sea to RIYD, which primarily sample the Arabian Shield, are faster than paths from the Zagros and Gulf of Aden which sample the Arabian Platform.

In this article, we present analysis of regional waveforms recorded by the 1995-1997 Saudi Arabian Broadband Deployment. From these data, we infer pure-path velocity structures for the Arabian Shield and Arabian Platform. We estimate velocity models by fitting the observed regional waveforms. We use a new method to expedite the waveform modeling grid search by first modeling the observed surface wave group velocities. Resulting lithospheric velocity models reveal significant structural differences between the shield and platform paths. The velocity structures we report for these regions provide new insights into the structure and composition of the Arabian Peninsula.

Data

Between November 1995 and March 1997 nine temporary broadband three-component seismic stations were deployed across central Saudi Arabia (Figure 1, we show only the six stations which had high quality data for the events studied). The stations were located primarily on the Arabian Shield. Studies using these data report significant differences in the character of the western and eastern Arabian Peninsula from short-period regional phase propagation (Mellors et al., 1998; Walter and McNamara, 1997) and surface wave group velocity dispersion (McNamara, Hazler and Walter, 1997; Mokhtar et al., 1997; Ritzwoller and Levshin, 1998; Pasyanos et al.,

1998). Using stacked short-period regional seismograms, Mellors et al. (1998) report that mantle body-wave phases (Pn and Sn) are much weaker than Lg for the Gulf of Aqaba and Syrian events observed at the Saudi Arabian temporary stations. Regional phase amplitudes for the Zagros to Saudi paths are more typical of stable continental areas. They also show that short-period Lg propagates very efficiently and the Lg velocities are faster for the Shield paths relative to the Platform paths suggesting that crustal Q and shear velocities are high in the Shield, respectively. Estimates of lithospheric velocity and discontinuity structure beneath the temporary stations from teleseismic receiver functions are reported by Sandvol et al. (1997). They report that crustal thickness is about 40-45 km and the average crustal shear wave velocity is about 3.7 km/s beneath the stations in the central Arabian Shield.

Two moderately large earthquakes recorded by the temporary stations provide excellent pure-path sampling of the Arabian Shield and the Arabian Platform (Figure 1). Event locations and origin times are taken from the USGS Preliminary Determination of Epicenters. Double-couple focal mechanisms and scalar moments are taken from the Harvard CMT catalog. Event depths were adjusted by fitting the regional waveforms using our best-fitting velocity models. Table 1 complies the event parameters.

Group Velocity Modeling

Surface wave group velocities in the period band 10-50 seconds are sensitive to lithospheric structure, especially crustal thickness and S-wave velocities. Because of the broad depth sampling of surface waves, group velocities are not uniquely related to velocity structure, but are more sensitive to the average velocity-depth profile. We modeled the observed group velocities to determine candidate velocity structures for grid search waveform modeling. The complete regional waveforms contain the body-waves and the surface wave group and phase velocity information and thus have greater sensitivity to lithospheric velocity structure. Because of non-uniqueness between

surface wave group velocities and seismic velocity structure and problems with group velocity measurement (e.g. measurement uncertainties, low signal-to-noise, spectral notches), estimates of velocity structure based solely on group velocity dispersion curves are probably not as accurate as those derived from waveform modeling. In fact, we found that models that fit the group velocity curves the best do not necessarily fit the observed waveforms as well as other models. Therefore, while group velocities provide some constraint on the velocity model, waveform matching provides tighter restrictions on the model because phase and amplitude information are included.

Differences between the structure of the Arabian Shield and Platform are immediately apparent from the Love and Rayleigh wave group velocity dispersion curves shown in Figure 2. Group velocities were measured from instrument deconvolved displacement seismograms using a multiple filter analysis code (C. Ammon, personal communication). Rayleigh and Love wave dispersion was measured on the vertical and transverse components, respectively. The curves are plotted only for periods where the surface wave amplitudes are not impacted by notches in the amplitude spectrum and/or poor signal-to-noise. This is why the Rayleigh wave group velocity curve for the Aqaba to Saudi path is cut at about 23 seconds. Uncertainties are ad hoc and set to the 90% reduction in amplitude of the frequency-time surface at each period. The observed dispersion curves show great differences between the Shield and Platform paths, with the Shield being about 10% faster. These variations in group velocity are similar to those obtained by Mokhtar and Al-Saeed (1992), McNamara, et al. (1997), Mokhtar, et al. (1997), Ritzwoller and Levshin (1998) and Pasyanos, et al. (1998).

Estimates of the velocity structure of the two regions resulted from modeling the observed group velocity dispersion with a grid search scheme. We generated a wide range of models and the Love and Rayleigh wave group velocity dispersion was computed for each model. The calculation of surface wave dispersion is very fast - much faster than that for a complete synthetic seismogram

computed with the reflectivity method. We evaluated the performance of each model by computing the combined Love and Rayleigh wave group velocity misfit using the L2-norm.
We chose to fit the band 15-45 seconds because this period range is most sensitive to the structure of the crust and uppermost mantle. At periods shorter than 15 seconds the group velocity measurements can be biased by low amplitude signals and scattered energy. The sediment thickness and upper crustal velocities control the short-period group velocities. Generally, the shape of the group velocity curve is controlled by the crustal thickness and velocity gradient. The velocity structure of the uppermost mantle, that controls the long-period behavior, was estimated by fitting the body-wave phase arrivals, Pn and Sn, by waveform modeling (see next section).

Independent constraints on lithospheric velocity structure helped to fit the observed group velocities and waveforms. We used models of sediment thickness and crustal thickness for the Arabian Peninsula (Cornell University Middle East North Africa Project, Seber, et al., 1997). These models are based on a large set of drill data, seismic reflection/refraction and gravity surveys. The sediment thickness is better constrained than crustal thickness. Deep sediments are present in the Arabian Gulf, but they gradually thin towards the Arabian interior. The crust is predicted to be 30-35 km near the Gulf of Aqaba and Red Sea and thickens to 40-45 km in central Arabia. Profiles generated through the Cornell models for the paths shown in Figure 1 provided averages of sediment and crustal thickness. The Platform paths are characterized by average sediment and crustal thicknesses of 4 km and 40 km, respectively. The average sediment thickness for the Arabian Shield paths is very low (< 1 km). Crustal thickness profiles for the Aqaba to Saudi paths are more variable (mean Moho depth of 32 km for the path to SODA and 42 km for the path to RAYN). Analysis of refraction data indicates the presence of a mid-crustal discontinuity in the Shield at about 20 km depth (Gettings et al., 1986). The sub-Moho P-wave velocity in the vicinity of the broadband stations is estimated to be 8.1 km/s (Gettings et al., 1986; Mellors et al., 1998). We fixed the sediment thickness (as stated above), the thickness of the lower crustal layer (20 km) and sub-Moho P- and S-wave velocities (8.10 and 4.55 km/s, respectively) for the group velocity

modeling grid search. The P- to S-wave velocity scaling was determined by setting Poisson's ratio to 0.25 in the crust and 0.27 in the mantle (Christensen and Mooney, 1995).

Three parameters were varied in the group velocity grid search: crustal thickness and the velocities of an upper and lower crustal layer. Given the above stated constraints, we generated models which spanned a broad range of the parameter space and evaluated the performance of each model. Crustal thickness varied from 34-48 km, with an increment of 2 km; upper crustal P-wave velocity varied from 5.8-6.5 km/s with an increment of 0.1 km/s and the lower crustal P-wave velocity varied from 6.2-7.2 km/s with an increment on 0.1 km/s. The range of models (704 total) along with the 10 best-fitting models are shown in Figure 3 for the Zagros-AFIF path. Notice that the ten best-fitting models have similar velocities in the upper crustal layer (6.2-6.3) and the lower crustal velocity and crustal thickness trade-off to roughly maintain a constant vertical travel time in the crust. The fit of the ten best models to the group velocities observed at AFIF are also shown in Figure 4. These models have remarkably similar dispersion curves and fit the data nearly equally well. A key result from Figures 3 and 4 is that the group velocities can constrain the velocities of the upper crust, but cannot simultaneously resolve the velocity of the lower crust and the crustal thickness.

Figure 2 shows the observed and predicted group velocity curves for the best-fitting models that resulted from both group velocity and waveform modeling (described below). The group velocity curves are well fit, however the large measurement uncertainties and the results of Figures 3 and 4 suggest that the observed curves can be fit by a wide variety of models.

Waveform Modeling

We modeled the observed waveforms to estimate the average one-dimensional seismic velocity structure of the Arabian Shield and Platform. The goal of this procedure is to determine a

velocity model which predicts the arrival times and amplitudes of the main regional body-wave phases (Pn, Pnl and Sn) and the Love and Rayleigh surface waves. Matching the observed waveforms with complete synthetic seismograms provides a more robust estimate of the structure than matching the observed group velocity dispersion alone. This is because the waveforms contain both the surface wave group and phase velocity information as well as the body-wave arrivals and relative amplitudes of body-to-surface waves.

Waveforms were fit using a grid search scheme similar to previous studies (Rodgers and Schwartz, 1998). Synthetic seismograms were calculated for many velocity structures using the reflectivity method (Randall, 1994). We expedited the waveform fitting process by limiting the grid search to those models that fit the group velocity dispersion roughly within the measurement uncertainties. The sediment thickness, lower crustal thickness and sub-Moho velocities were held constant in the waveform modeling grid search, similar to the group velocity modeling. We set shear wave attenuation in the crust to values consistent with those reported by Seber and Mitchell (1992): $Q_S = 80$ in the sediment layer and upper crust and $Q_S = 150$ elsewhere. We set compressional wave attenuation to 9/5 times the shear wave attenuation. Consistent with Seber and Mitchell (1992) we found that crustal attenuation does not strongly affect the observed amplitudes for periods greater than about 10 seconds. Figure 5 shows the velocity models used in the waveform modeling grid search for the Zagros-Saudi path. In these models crustal thickness varied from 38-44 km, with an increment of 2 km; upper crustal P-wave velocity varied from 6.0-6.4 km/s with an increment of 0.1 km/s and the lower crustal P-wave velocity varied from 6.2-6.8 km/s with an increment on 0.1 km/s. These parameter values resulted in 140 models. We measured model performance with the combined three-component L2-norm misfit. The five best-fitting models are also shown in Figure 5. Note that the lower crustal velocity and crustal thickness trade-off similar to the group velocity modeling grid search (Figure 3). However, the upper crustal velocity estimated from waveform modeling are very close to that estimated from group velocity modeling.

The model for the Shield paths obtained from waveform modeling is shown in Figure 6 and the fits to the three-component waveforms recorded at AFIF are shown in Figure 7a. Because of weak long-period Rayleigh wave excitation, we included short-periods down to 10 seconds. The Love and Rayleigh waves are well fit by the Arabian Shield model. Crustal thickness is 36 km and average P- and S-wave crustal velocities are 6.42 and 3.70 km/s, respectively. However the body-wave phases Pn and Sn on the vertical and radial components are not particularly well fit. In order to fit the relative timing of these arrivals, we had to decrease the sub-Moho P- and S-wave velocities to 7.9 and 4.30 km/s, respectively, corresponding to a high upper mantle Poisson's ratio of 0.29. These portions of the waveform could be poorly fit due to either focal mechanism errors (Sn is near nodal), attenuation or crustal thickness variations along the path. It is well established from refraction and receiver function analysis that the crust is about 40 km thick and relatively fast beneath the temporary stations (Gettings et al., 1985; Sandvol, et al., 1997). The Cornell crustal model (Seber et al., 1997) indicates that the crust is 30-35 km thick in the Gulf of Aqaba. Variations in the crustal thickness at the source and receiver will affect the body-waves and surface waves differently. We chose to fit the surface waves, and we attribute the poor fit to the body-waves as a possible focal mechanism and/or propagation effect due to non-plane layered structure.

The observed three-component component seismograms and synthetics for the best-fitting velocity model for the Arabian Platform (Zagros-Saudi paths) are shown in Figure 7b. Data and synthetics were filtered 20-100 seconds. The body-wave and surface waves are generally well fit by the synthetics. Note that long-period noise affects the radial component near the Pnl arrival, however the vertical component is relatively noise free. The Platform Model is shown in Figure 6. The best fitting model has a crustal thickness of 40 km and crustal velocities are relatively slow (average P- and S-wave velocities of 6.07 and 3.50 km/s, respectively). The mantle velocities are typical of stable continental regions (P- and S-wave velocities of 8.10 and 4.55 km/s, respectively), with a normal mantle Poisson's ratio of 0.27 (Christensen and Mooney, 1995).

Figure 2 shows the fit of the group velocities predicted by the models estimated from waveform modeling to the observed group velocities. It is important to note that models that provide good fits to the observed waveforms predict the group velocity dispersion within the uncertainty estimates. However, the models which gave the best fits to the observed group velocity dispersion do not necessarily fit the observed waveforms as well. Synthetics for these models misfit the surface wave phase, suggesting that modeling both group and phase velocities simultaneously will result in better fits to the waveforms. The crustal thickness and crustal velocities inferred from group velocity and waveform modeling are remarkably close for the Shield paths, but less so for the Platform path. This indicates that the group velocities provide valuable constraints on initial models and can be used to expedite the waveform fitting process. Especially encouraging is the agreement between the upper crustal velocities estimated from group velocity and waveform modeling. Because the group velocity calculation is roughly 20 times faster than the synthetic seismogram calculation, the time savings benefit of constraining the waveform modeling parameter space with the results of group velocity modeling is substantial. Also, the computation time saved can be spent investigating more detailed crustal structure (e.g. sediment layer structure, crustal velocity gradients) with waveform modeling.

Discussion - Lithospheric Composition and Tectonic Implications

The velocity structures inferred from the above analysis require significantly different lithospheric compositions which must have resulted from different tectonic evolution. The main differences between the crustal velocity profiles of the two regions (Figure 6) are the excess sediments, the absence of a high velocity lower crust and the thicker crust in the Arabian Platform. These differences in velocity structure cannot be explained by a single crustal structure overlain with additional sediment on the Arabian Platform. Low crustal velocities in the Platform indicate a primarily felsic composition while the faster velocities of the Shield indicate a mafic lower crust (Christensen and Mooney, 1995). Felsic composition of the Platform is consistent with orogenesis

of this former active margin in late Proterozoic times (Stoeser and Camp, 1985). It is interesting to note that the waveforms are best fit by a relatively uniform crust, whereas the group velocities prefer a velocity increase with depth. It is possible that our preferred Platform model is simple because we're fitting the longer period (20 seconds and higher) surface waves. An important difference between waveform modeling and group velocity modeling is that group velocities are modeled with all frequencies being weighted equally, however waveforms have some frequencies more strongly represented than others due to source excitation and propagation effects. For example, a 20 second Rayleigh wave (the Airy phase) is typically the largest amplitude surface wave for continental paths. When the waveform misfit is measured by the L2-norm, the Airy phase will dominate the sensitivity of the data to the structure at the expense of the smaller amplitude body-waves or long-period surface waves. When periods as short as 10 seconds were included, we estimated a similar model. Regardless of which period band was used to estimate the velocity structure, the average crustal velocities for the Platform paths are low and there is no suggestion of a strong velocity gradient.

Average crustal velocities for our Arabian Shield model are slightly slower than that from previous, more localized studies (e.g. Gettings, et al., 1986; Sandvol et al., 1998; Al-Amri, 1998). This may arise due to slower along-path velocities near the Gulf of Aqaba or beneath the volcanic centers. The Shield model includes a strong velocity increase between the upper and lower crust. The high velocities in the lower crust of the Arabian Shield suggest a mafic composition at depth. This is consistent with the island arc origin of the western most terranes of the Shield. The presence of volcanics on the Arabian Shield may have resulted in mafic addition to the crust, which would increase bulk crustal velocities. A bulk mafic composition would result in a higher than average crustal Poisson's ratio (> 0.27). Unfortunately the Pnl wave is poorly excited for the Aqaba event preventing us from obtaining a good estimate of the crustal P-wave velocity for this path. The observation that the crustal velocities are rather fast and that short-period Lg waves are not strongly attenuated suggests that partial melt associated with volcanism is not wide spread throughout the crust in western Arabia. However, from the paths used in this study we cannot

determine the lateral extent of any anomalous zone. The low sub-Moho velocities, high Poisson's ratio (0.29) in the shallow mantle, the absence of efficient short-period Sn in the Arabian Shield (Mellors et al., 1998) and the presence of volcanic centers are all consistent with the presence of partially molten mantle directly beneath the Moho.

Finally, the inferred seismic velocity structures have implications for the mass balance of the Arabian Peninsula. The Arabian Shield is topographically higher on average than the Arabian Platform, yet the crust is thinner beneath the Shield. Furthermore, the inferred crustal velocities imply that the Shield crust is more dense than the Platform. The higher topography of the Shield could be supported in part by less dense, low velocity mantle. While we cannot directly infer dynamical properties of the Arabian Shield, our results are broadly consistent with hot, upwelling asthenosphere as reported by Camp and Roobol (1992) based on analysis of volcanic rocks. Future investigations using broadband seismic data from a dense network will provide further insights into the structure of this complex region.

Acknowledgments

This study would not be possible without the data collection and organization efforts of Frank Vernon and colleagues from the University of California, San Diego. Group velocity dispersion was measured using programs written by Charles Ammon of Saint Louis University. Models of basalt cover, sediment and crustal thickness were provided by Eric Sandvol, Dogan Seber and Muawia Barazangi of Cornell University. Comments by Victor Camp and Steve Myers are gratefully acknowledged. Careful reviews by Eric Sandvol and Mark Gettings and editorial assistance from Steve Ward improved the original manuscript. This work was performed in part under the auspices of the U.S. Department of Energy by the Lawrence Livermore National Laboratory under contract W-7405-ENG-48. This is LLNL contribution UCRL-JC-132098. This

is contribution number 388 of the W M Keck Seismological Laboratory and the Institute of Tectonics, University of California, Santa Cruz.

References

Al-Amri, A. M. S., 1998. The crustal structure of the western Arabian platform from the spectral analysis of long-period P-wave amplitude ratios, *Tectonophysics,* **290**, 271-283.

Al-Amri, A. M. S., 1999. The crustal and upper-mantle structure of the interior Arabian platform, *Geophys. J. Int.*, **136**, 421-430.

Camp, V. and M. Roobol, 1992. Upwelling asthenosphere beneath western Arabia and its regional implications, *J. Geophys. Res.*, **97**, 15,255-15,271.

Christensen, N. and W. Mooney, 1995. Seismic velocity structure and composition of the continental crust: A global view, *J. Geophys. Res.*, 100, 9761-9788.

Gettings, M., H. Blank, W. Mooney and J. Healey, 1986. Crustal structure of southwestern Saudi Arabia, *J. Geophys. Res.*, **91**, 6491-6512.

McNamara, D., S. Hazler and W. Walter, 1997. Velocity structure across northern Africa, southern Europe, the Middle East and the Arabian Peninsula from surface wave dispersion, *EOS*, **78**, F499.

Mellors, R., F. Vernon, V. Camp, A, Al-Amri, A. Gharib and M. Al-Dial, 1998. Regional waveform propagation in the Saudi Arabian Peninsula, preprint.

Moktar, T. and M. Al-Saeed, 1994. Shear wave velocity structures of the Arabian Peninsula, *Tectonophysics*, **230**, 105-125.

Moktar, T., C. Ammon, H. Ghalib, and R. Herrmann, 1997. Lithospheric structure beneath Arabia, *EOS*, **78**, F499.

Pasyanos, M., W. Walter, S. Hazler and D. McNamara, 1998. Surface wave research in the Middle East and North Africa, Proceedings for the 20th Annual Seismic Research Symposium on Monitoring a Comprehensive Test Ban Treaty, 21-23 September, 1998.

Randall, G., 1994. Efficient calculation of complete differential seismograms for laterally homogeneous earth models, *Geophys. J. Int.*, **118**, 245-254.

Ritzwoller, M. and A. Levshin, 1998. Eurasian surface wave tomography: Group velocities, *J. Geophys. Res.*, **103**, 4839-4878.

Rodgers, A., and S. Schwartz, 1998. Lithospheric structure of the Qiangtang Terrane, northern Tibetan Plateau, from complete regional waveform modeling: evidence for partial melt, *J. Geophys. Res.*, **103**, 7137-7152.

Sandvol, E., D. Seber, M. Barazangi, F. Vernon, R. Mellors and A. Al-Amri, 1998. Lithospheric velocity discontinuities beneath the Arabian Shield, *Geophys. Res. Lett.*, **25**, 2873-2876.

Seber, D. and B. Mitchell, 1992. Attenuation of surface waves across the Arabian Peninsula, *Tectonophysics*, **204**, 137-150.

Seber, D., M. Vallve, E. Sandvol, D. Steer and M. Barazangi, 1997. Middle East tectonics: applications of geographical information systems (GIS), *GSA Today*, February 1997, 1-5.

Stoeser, D. and V. Camp, 1985. Pan-African microplate accretion of the Arabian shield, *Geol. Soc. Am. Bull.*, **96**, 817-826.

Walter, W. and D. McNamara, 1997. Propagation characteristics of Lg throughout the Middle East, Mediterranean, southern Europe and northern Africa, *EOS*, **78**, F499.

Tables

Table 1. Source parameters of events used in this study. Events are identified in Figure 1 by their year and day of year (yy_ddd).

Event	Origin Time (GMT)	Latitude	Longitude	Depth (km)	m_b	Strike/Dip/Rake
95_327	1995 Nov. 23 (327) 18:07:17.3	29.333°	34.749°	20	5.2	199°/77°/7°
96_145	1996 May 25 (145) 06:35:58.7	27.847°	53.594°	5	4.9	107°/22°/88°

Table 2. Arabian Shield and Platform lithospheric velocity models.

Arabian Shield Model			**Arabian Platform Model**		
thickness (km)	v_P (km/s)	v_S (km/s)	thickness (km)	v_P (km/s)	v_S (km/s)
1	4.0	2.31	4	4.0	2.31
15	6.2	3.58	16	6.2	3.64
20	6.8	3.93	20	6.4	3.70
∞	7.9	4.30	∞	8.1	4.55

Figure Captions

Figure 1. Map of the Arabian Peninsula showing the locations of the earthquakes (circles), stations (triangles) and paths (gray lines) considered. The heavy black line marks the approximate boundary between the sediment cover of the Arabian Platform and the exposed basement of the Arabian Shield. The gray shading indicates neogene-Quaternary basalt cover.

Figure 2. Love (top) and Rayleigh (bottom) wave group velocity dispersion curves and errors for the Aqaba (circles) and Zagros (squares) paths to stations AFIF and HALM. The thin lines are the group velocity curves for the models which provide the best fits to the group velocities. The thick lines are the group velocity curves for the preferred models which provide the best fit to the complete waveforms.

Figure 3. The S- and P-wave velocity models used in the group velocity grid search for the Zagros-AFIF path (gray lines). Values of the model parameters are given in the text. Also shown are the ten best-fitting models (black lines).

Figure 4. Observed group velocities for the Zagros-AFIF path (squares with error bars) and the fits of the ten best models shown in Figure 3.

Figure 5. The S- and P-wave velocity models used in the waveform modeling grid search for the Zagros-AFIF path (gray lines). Values of the model parameters are given in the text. Also shown are the five best-fitting models (black lines).

Figure 6. The Arabian Shield (black) and Platform (gray) velocity models. The thick lines are the preferred models which provide the best fit to the waveforms. The thin lines are the models which provide the best fits to the group velocities.

Figure 7. (a) Observed three-component waveforms (solid) for the Aqaba event (filtered 10-100 seconds) and synthetics for the Arabian Shield model (dashed). (b) Same as (a) but for the Zagros event (filtered 20-100 seconds) and Arabian Platform model.

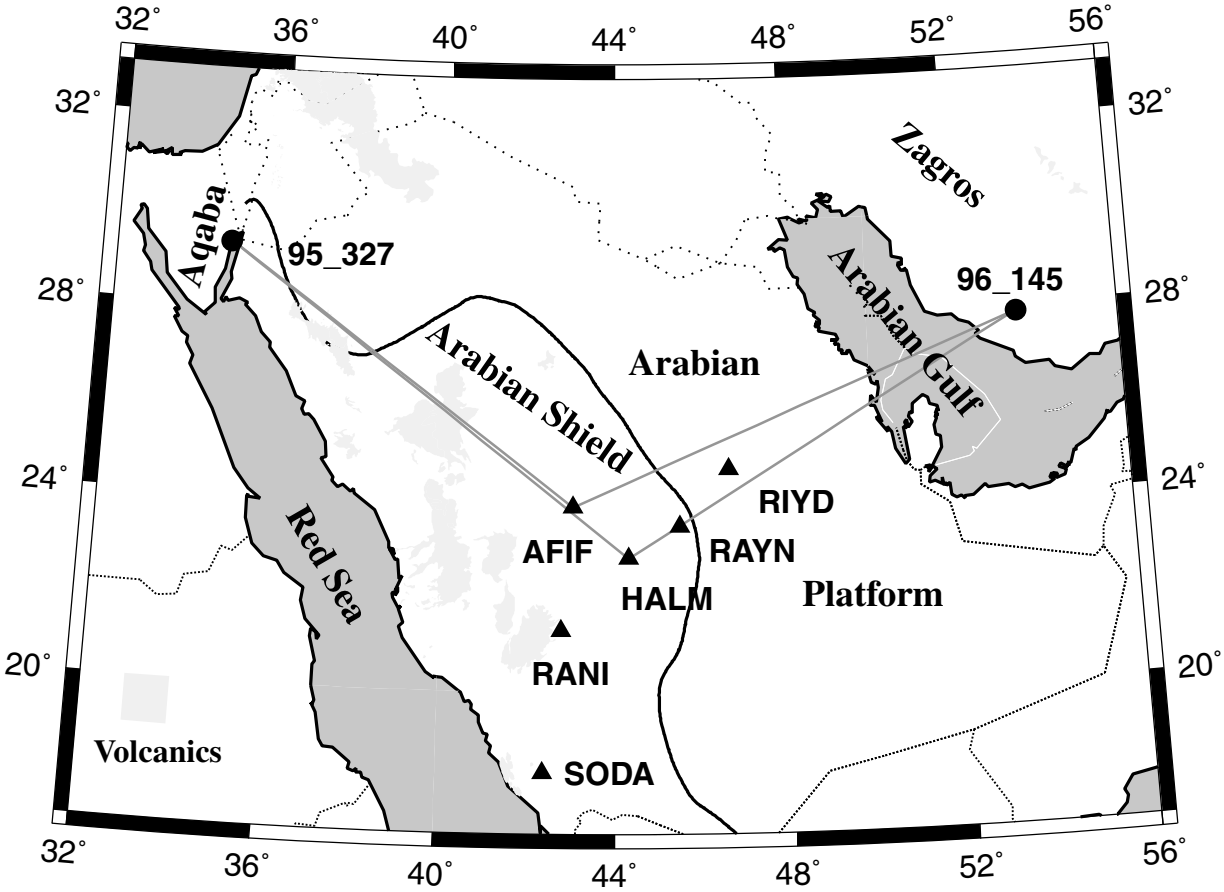

Rodgers et al., 1998, Arabian Lithospheric Structure, Figure 1

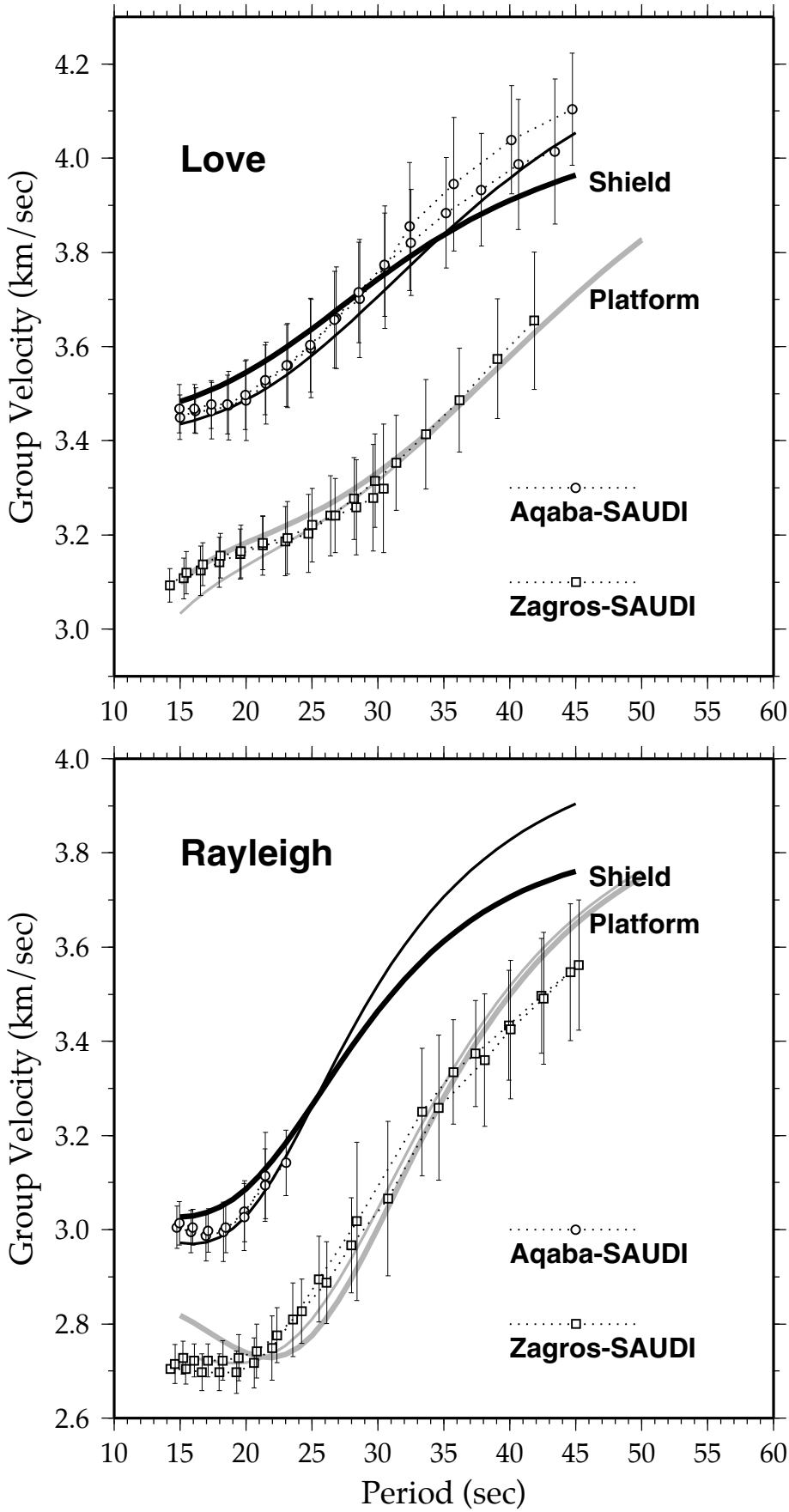

Rodgers et al., 1999, Arabian Lithospheric Structure, Figure 2

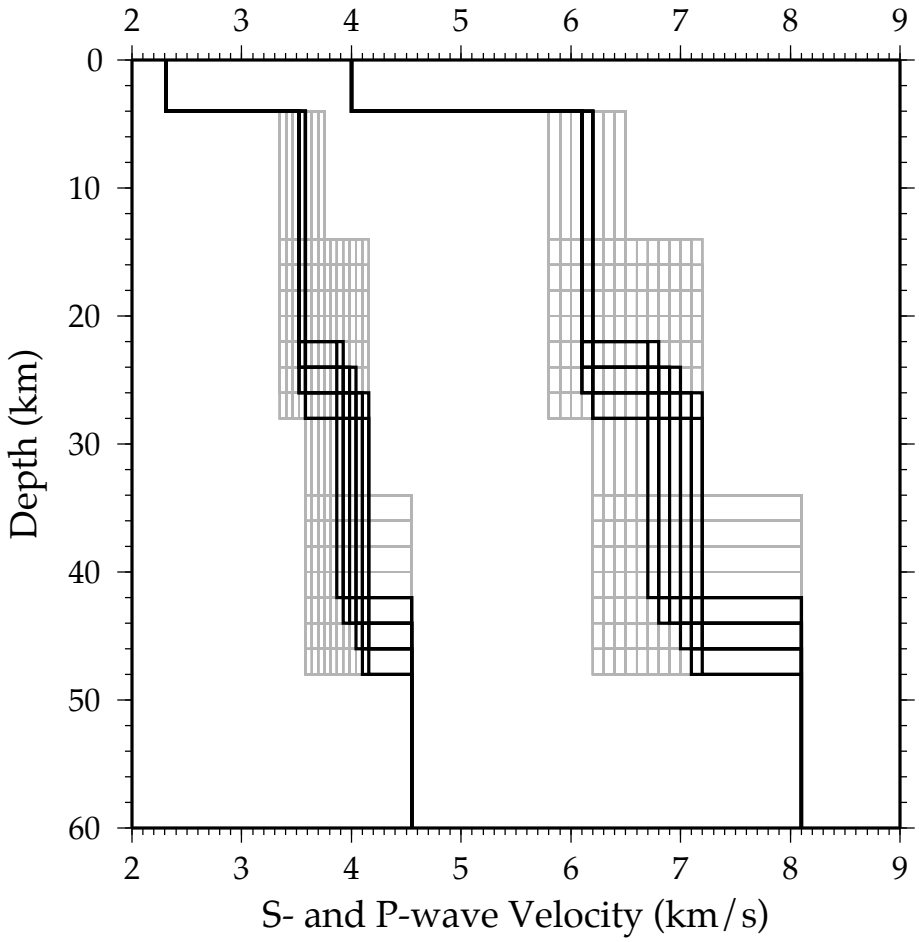

Rodgers et al., 1999, Arabian Lithospheric Structure, Figure 3

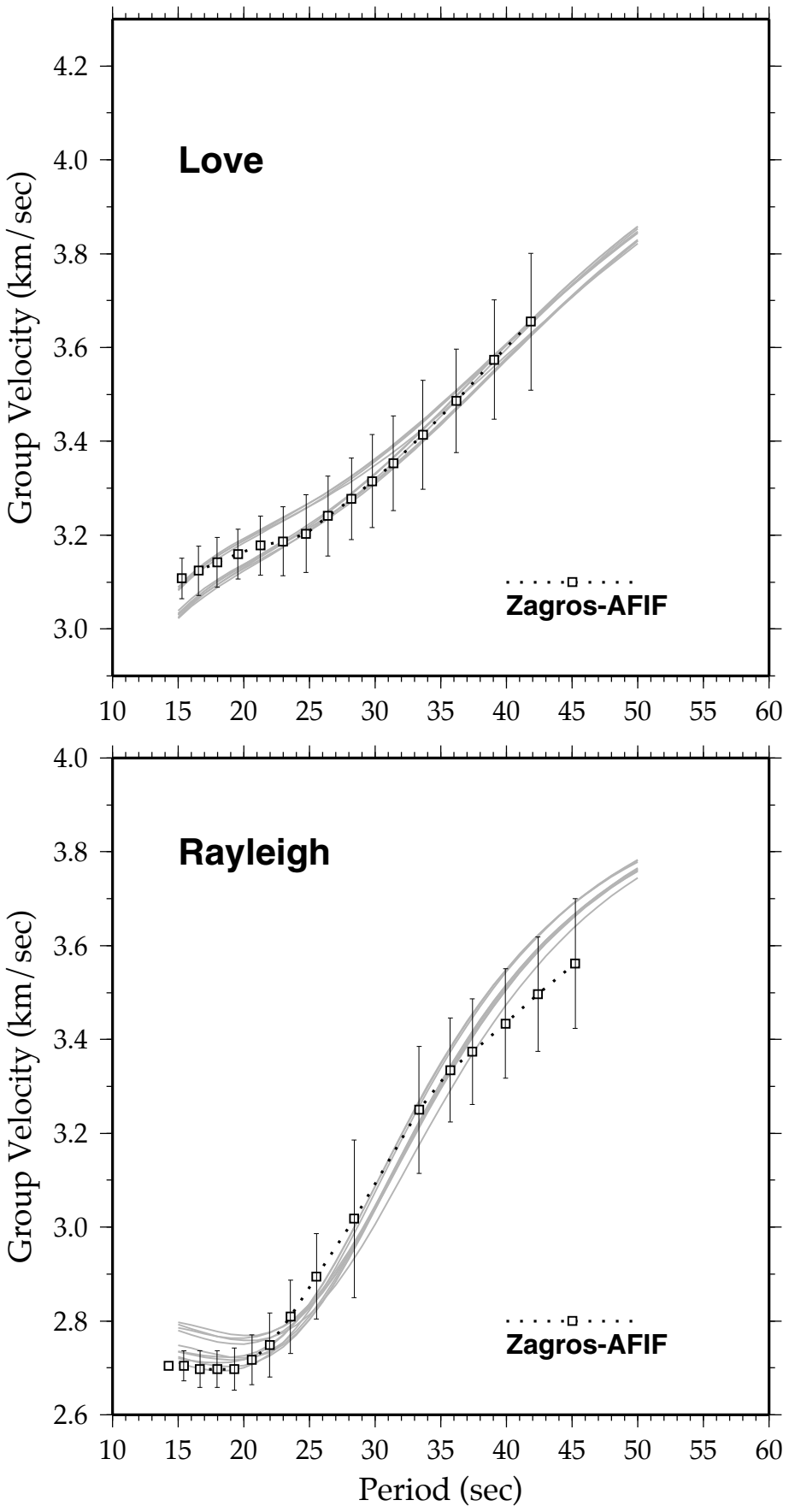

Rodgers et al., 1999, Arabian Lithospheric Structure, Figure 4

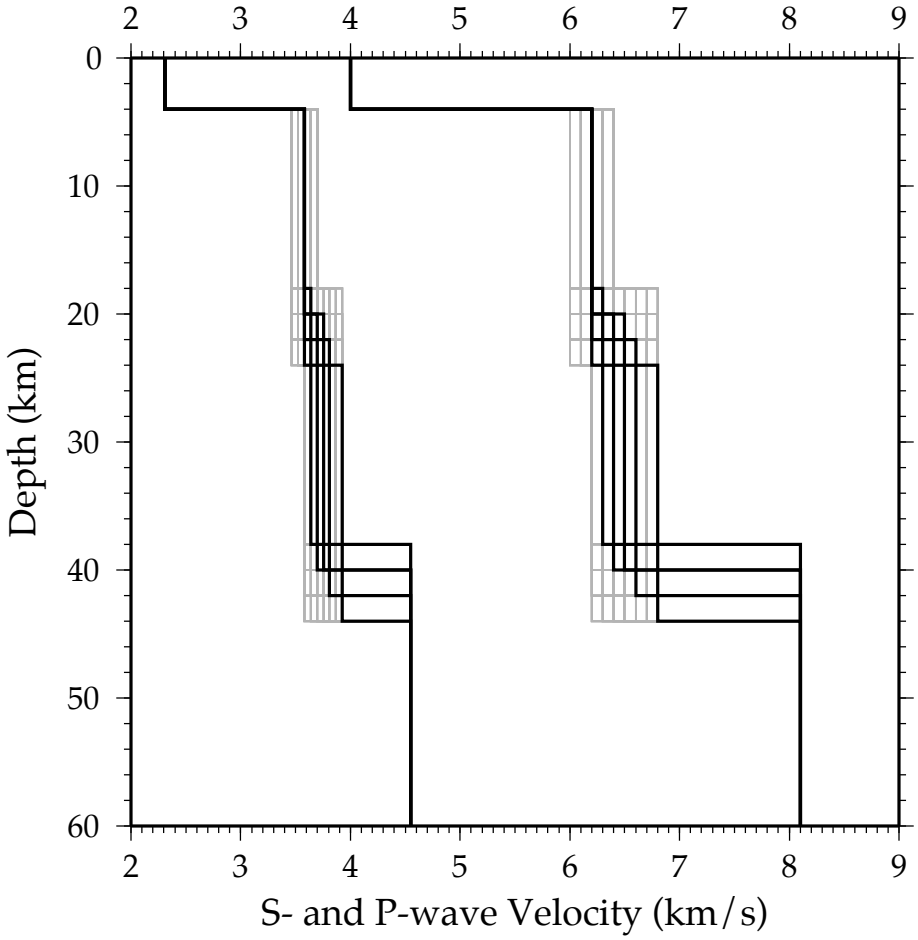

Rodgers et al., 1999, Arabian Lithospheric Structure, Figure 5

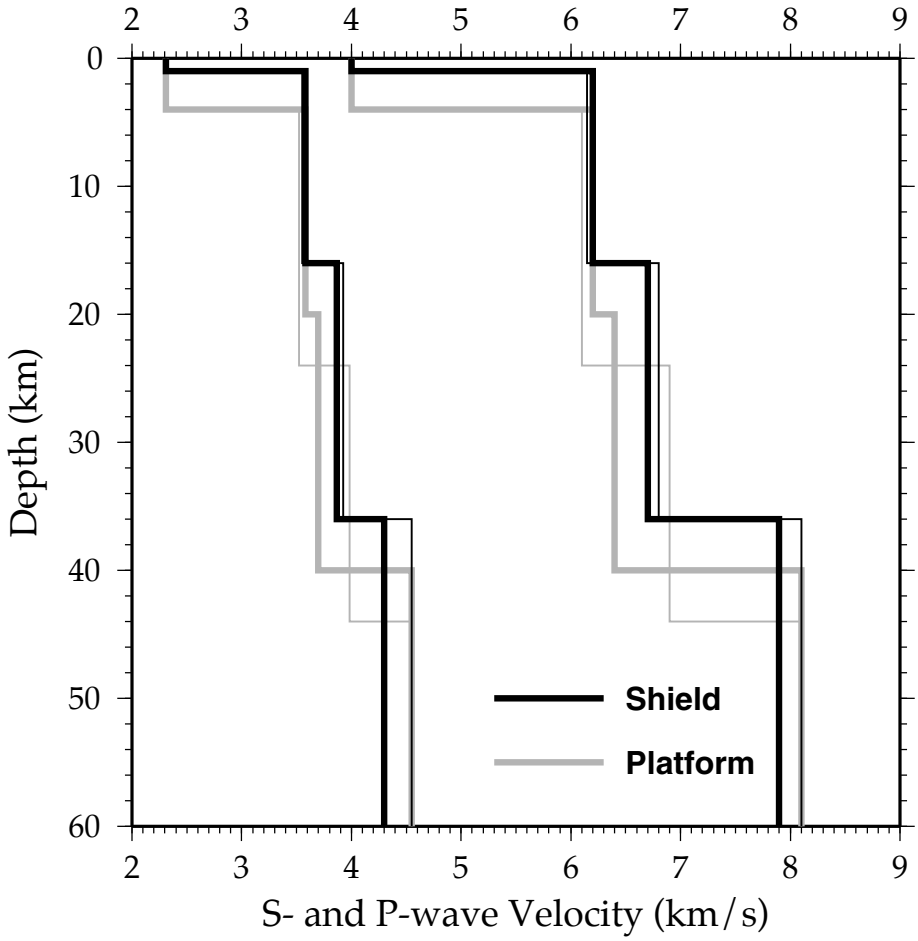

Rodgers et al., 1999, Arabian Lithospheric Structure, Figure 6

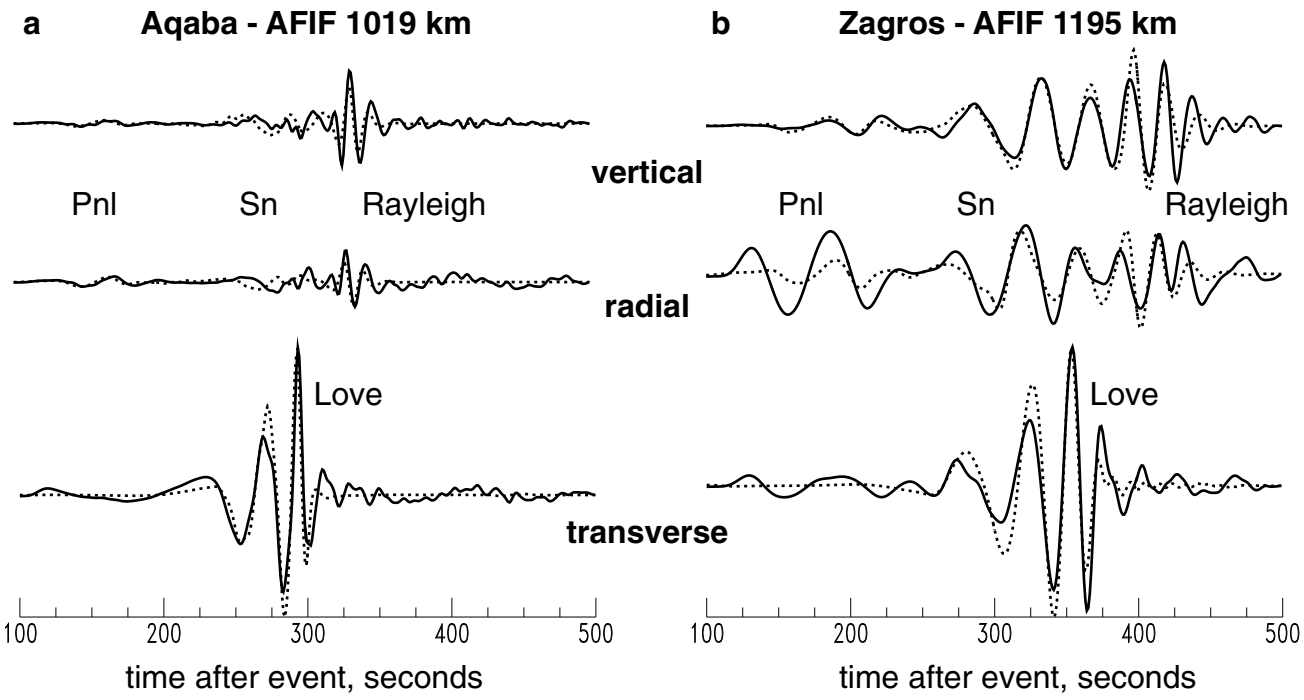

Rodgers et al., 1999, Arabian Lithospheric Structure, Figure 7